AGU PUBLICATIONS

Geophysical Research Letters

RESEARCH LETTER
10.1002/2015GL065061

Key Points:
- Extreme induced geoelectric field characteristics
- Evidence of localized geoelectric field peak enhancements
- Physical drivers of localized fields not clear

Supporting Information:
- Readme
- Movie S1
- Movie S2
- Movie S3
- Movie S4
- Movie S5
- Movie S6
- Movie S7
- Movie S8
- Movie S9
- Movie S10
- Movie S11
- Movie S12
- Movie S13
- Movie S14
- Movie S15
- Movie S16
- Movie S17
- Movie S18
- Movie S19
- Movie S20
- Movie S21
- Movie S22
- Movie S23
- Movie S24

Correspondence to:
C. M. Ngwira,
chigomezyo.ngwira@nasa.gov

Citation:
Ngwira, C. M., A. A. Pulkkinen, E. Bernabeu, J. Eichner, A. Viljanen, and G. Crowley (2015), Characteristics of extreme geoelectric fields and their possible causes: Localized peak enhancements, *Geophys. Res. Lett.*, *42*, doi:10.1002/2015GL065061.

Received 25 JUN 2015
Accepted 14 AUG 2015
Accepted article online 18 AUG 2015

Characteristics of extreme geoelectric fields and their possible causes: Localized peak enhancements

Chigomezyo M. Ngwira[1,2], Antti A. Pulkkinen[2], Emanuel Bernabeu[3], Jan Eichner[4], Ari Viljanen[5], and Geoff Crowley[6]

[1]Department of Physics, Catholic University of America, Washington, District of Columbia, USA, [2]Space Weather Laboratory, NASA Goddard Space Flight Center, Greenbelt, Maryland, USA, [3]PJM Interconnection, Audubon, Pennsylvania, USA, [4]Munich Re, Geo Risks Research, Munich, Germany, [5]Finnish Meteorological Institute, Helsinki, Finland, [6]Atmospheric and Space Technology Research Associates, Boulder, Colorado, USA

Abstract One of the major challenges pertaining to extreme geomagnetic storms is to understand the basic processes associated with the development of dynamic magnetosphere-ionosphere currents, which generate large induced surface geoelectric fields. Previous studies point out the existence of localized peak geoelectric field enhancements during extreme storms. We examined induced global geoelectric fields derived from ground-based magnetometer recordings for 12 extreme geomagnetic storms between the years 1982 and 2005. For the present study two important extreme storms, 29 October 2003 and 13 March 1989, are shown. The primary purpose of this paper is to provide further evidence on the existence of localized peak geoelectric field enhancements and to show that the structure of the geoelectric field during these localized extremes at single sites can differ greatly from globally and regionally averaged fields. Although the physical processes that govern the development of these localized extremes are still not clear, we discuss some possible causes.

1. Introduction

One of the key requirements for the analysis of risks posed by geomagnetically induced currents (GIC) is a specification of the geoelectric field at spatial scales relevant for specific power network systems [e.g., *Pirjola*, 2002; *Bernabeu*, 2013; *Love et al.*, 2014]. In turn, it is a major challenge to understand the basic processes associated with the development of dynamic magnetosphere-ionosphere currents, which generate large induced geoelectric fields on the ground.

When considering system-wide space weather impacts, it is typically assumed that the extreme geoelectric fields covering the entire footprint of the power system are spatially uniform. However, it has recently been observed by these authors that at the time when the global geoelectric fields are enhanced, the extreme maxima in the field are actually localized, i.e., single station peak at least 100% larger than the regional (distances of the order of 500 km) average. The structure of the local geoelectric field during these extremes at single sites can differ greatly from globally and regionally averaged geoelectric fields [*Pulkkinen et al.*, 2015]. The physical processes that govern the generation of these extremes have not been sufficiently explored.

In our earlier study [*Pulkkinen et al.*, 2015], the spatial coherence of the geoelectric field was of particular interest, since it has not been considered enough. The primary purpose of the present paper is to build on our work in *Pulkkinen et al.* [2015] and expand our investigation on the existence of localized geoelectric field extremes. Both spatial coherence and localized enhancements are important when considering GIC effects and their impact. While there have been isolated reports of localized geomagnetic (GIC-related) events [e.g., *Boteler and Jansen van Beek*, 1999; *Pulkkinen et al.*, 2015], further evidence of events that produced localized extremes is provided here. We demonstrate the occurrence of localized extreme geoelectric fields with two specific examples and discuss some possible causes.

2. Data and Analysis

Global 60 s geomagnetic field data acquired from INTERMAGNET (www.intermagnet.org) were used for our investigation. The geoelectric field was computed using the measured geomagnetic field data from each geophysical observatory and the Quebec multilayer ground conductivity model [e.g., *Pulkkinen et al.*, 2012;

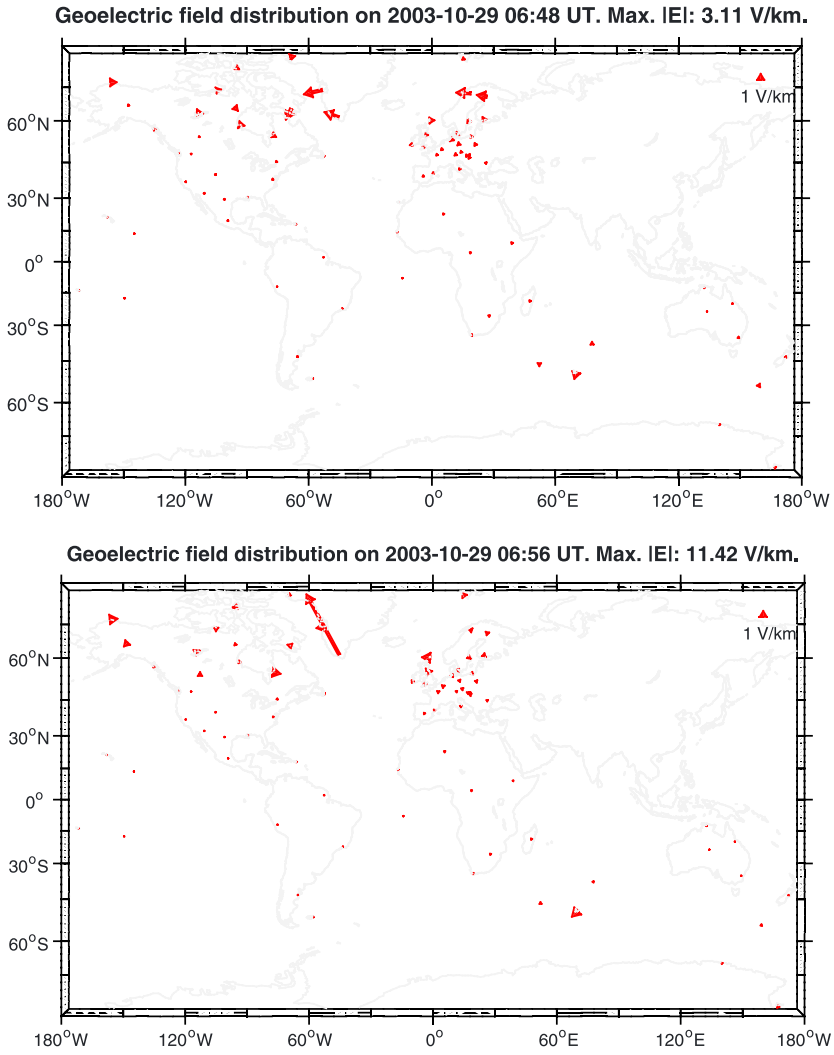

Figure 1. Calculated global geoelectric fields for 29 October 2003: (top) showing "nearly uniform" extreme geoelectric field enhancements and (bottom) showing extreme geoelectric field enhancement at Narsarsuaq, Greenland. Note that the maximum geoelectric field amplitude indicated on the top of the figures refer to a single station maximum.

Ngwira et al., 2013] by applying the local plane wave method, a well-established method for GIC applications [see, e.g., *Pirjola*, 2002; *Viljanen et al.*, 2006a]. The Quebec model is relatively resistive and is therefore a "conservative" choice for ground models, which is a preferred approach in dealing with the uncertainty inherent in our knowledge of the ground conductivity. In this study, we are primarily interested in the distribution of ionospheric currents that produce large fields. To a good approximation, the same ionospheric-magnetospheric source current will generate similar total geomagnetic field variations at regions having different ground conductivity structures. *Tanskanen et al.* [2001] show that a large portion of the geomagnetic variation is of external origin, and the difference in internal geomagnetic field magnitudes associated with different realistic conductivity structures is still quite small.

Since the focus of our study is on extreme events, only data for 12 of the most severe geomagnetic storms, based on the minimum *Dst*, that were observed during the period of 1982–2005 were examined (for a full description of the selection process, [see *Ngwira et al.*, 2013]). In the present study, two important extreme storms, 29 October 2003 and 13 March 1989, are specifically shown. For each event, the geoelectric field was computed at each time step for all available magnetometer stations, and thereafter, geoelectric field variations were visually analyzed using global distribution images, such as provided in Figure 1. A geoelectric field is classified as extreme if it exceeds 1 V/km. In *Pulkkinen et al.* [2015], a statistical study using the same method described above determined that geoelectric field values above 1 V/km are sufficiently rare to be considered

Table 1. List of Geomagnetic Events Analyzed for This Study Showing the Year, Month, Day, UT/Solar Local Time (LT), Peak Geoelectric Field (*E* Field), Latitude, Longitude, the Location of Localized Peak *E* Field Enhancements, and the *E* Field Dropoff Ratio (Peak *E* Field Divided by Maximum *E* Field of Nearest Site) and Separation Distance in Kilometers

Year	Storm Month	Day	Time UT (LT)	Peak *E* Field (V/km)	Latitude (Magnetic)	Longitude (Magnetic)	Location of Peak *E* Field	*E* Field Ratio/ Distance (km)
1982	07	13	00:01 (01:01)	6.59	56.5	95.8	Uppsala (UPS)	7.85/513
1989	03	13	21:46 (22:46)	5.91	53.1	90.2	Brorfelde (BFE)	10.02/287
			21:46 (21:46)	3.74	53.9	78.0	Eskdalemuir (ESK)	11.69/503
			21:46 (16:46)	1.57	50.5	357.1	Fredericksburg (FRD)	6.04/803
1991	03	24	04:04 (01:04)	4.0	85.8	31.9	Qaanaaq (THL)	9.75/1393
1991	11	08	22:13 (22:13)	3.93	53.9	78.0	Eskdalemuir (ESK)	9.14/503
2000	04	06	17:33 (07:33)	2.43	70.6	249.9	Barrow (BRW)	2.92/815
2000	07	15	14:40 (10:40)	2.79	73.6	14.2	Iqaluit (IQA)	2.54/1076
2001	03	31	01:02 (21:02)	2.24	73.6	14.2	Iqaluit (IQA)	2.55/1076
2001	11	06	05:24 (06:24)	1.62	65.3	101.7	Abisko (ABK)	2.19/344
2003	10	29	06:56 (03:56)	11.42	67.1	43.5	Narsarsuaq (NAQ)	11.20/1072
2003	11	20	08:11 (20:11)	5.07	65.8	263.1	College (CMO)	9.57/815
2004	11	07	18:30 (08:30)	1.86	70.6	249.9	Barrow (BRW)	5.03/815
2005	05	15	02:57 (11:07)	2.63	−80.1	325.1	Scott Base (SBA)	23.91/1600

extreme. We must stress that our original goal was not to identify "localized" geoelectric fields but rather to characterize the detailed global spatiotemporal variations of the induced peak geoelectric fields. However, as the data were analyzed, we observed that the localized peaks were a very common occurrence during all storm events.

In Table 1 a list of the events and their associated localized extreme peaks is provided, including information about the solar local times, specific INTERMAGNET locations of the peak geoelectric field enhancements, and the geoelectric field dropoff ratio (peak *E* field divided by maximum *E* field of nearest site at same time instance) over the separation distance in kilometers. The dropoff ratio is a measure of how quickly the peak geoelectric field decreases with distance. Clearly, the peak *E* field is more than 200% larger than the second highest peak value in each of the 12 events at the same time step of occurrence of the highest peak of each event. During any given storm (lasting around 3–36 h), the peak enhancements can occur at different locations and at different times as the storm progresses; however, the UT time and local time shown in the table indicate when the maximum field occurred during the entire storm period. Table 1 clearly shows that the time instances during which these extreme local peaks occur cover a wide range of local times. The events also appear at different latitudes.

Figure 1 displays images containing the geoelectric fields computed as outlined above for 29 October 2003. Figure 1 (top) displays an example of a geoelectric field distribution that is relatively uniform across the northeastern Canadian and Greenland area at 06:48 UT, while Figure 1 (bottom) shows a localized peak geoelectric field extreme in the southern part of Greenland at 06:56 UT. Figure 2 shows a second example of a localized extreme maximum in the geoelectric field that occurred at 21:46 UT during the storm on 13 March 1989. For this case (Figure 2), the localized extremes appear over two different higher midlatitude locations at Eskdalemuir (ESK) in UK and Brorfelde (BFE) in Denmark. We also note that another case of midlatitude localized enhancement appears at Fredericksburg (FRD) on the eastern coast of continental USA. Clearly, the localized effect in both examples above is confined to very specific areas rather than regional scales. This significantly deviates from the traditional, e.g., Figure 1 (top), storm time geoelectric field distribution pattern in which the regional variations are assumed to be more or less uniform [e.g., *Bernabeu*, 2013]. It should be noted that the local extremes are not limited to the Northern Hemisphere but occur in the Southern Hemisphere as well (see last event in Table 1). For the present study, however, we have selected marked events from the Northern Hemisphere because of the larger number of ground magnetometers, which allows better quantification of geoelectric field spatial scales associated with the events.

To further investigate the local extremes, an examination of the ground geomagnetic and geoelectric field response was performed. For each site considered, baselines were determined and subtracted from the

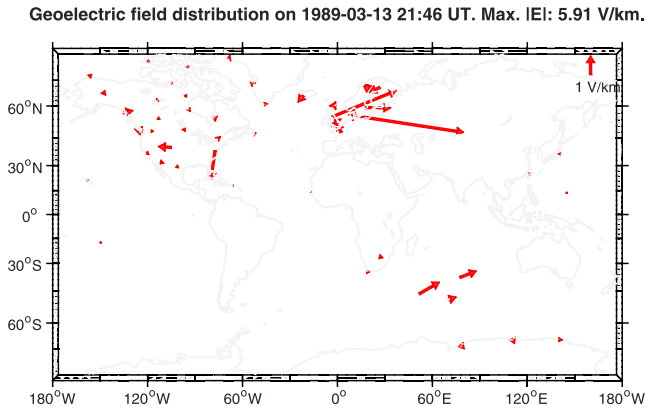

Figure 2. Example of global geoelectric fields showing localized enhancements at Eskdalemuir and Brorfelde geomagnetic stations in Europe and at Fredericksburg in USA during 13 March 1989 event. The vector scale in this figure is different from Figure 1 to clearly illustrate the enhancements.

geomagnetic observations. The baselines were derived by taking the quiet time mean values during the postmidnight period between 02 and 03 local time. In Figure 3 we present time series of the geomagnetic *X* component perturbations (top row), its rate of change (middle row), and the computed geoelectric fields (bottom row) for selected locations during the event on 13 March 1989. For this midlatitude case associated with the image in Figure 2, the sites shown are located at (Figure 3, left column) Lerwick (LER), ESK, Hartland (HAD), BFE, and Wingst (WNG) in Europe (nighttime) and (Figure 3, right column) Ottawa (OTT), St. John's (STJ), and FRD in North America (near sunset). Appearance of localized geoelectric field enhancements at 50° geomagnetic latitude (at FRD) shows that the events are not completely restricted to high-latitude auroral

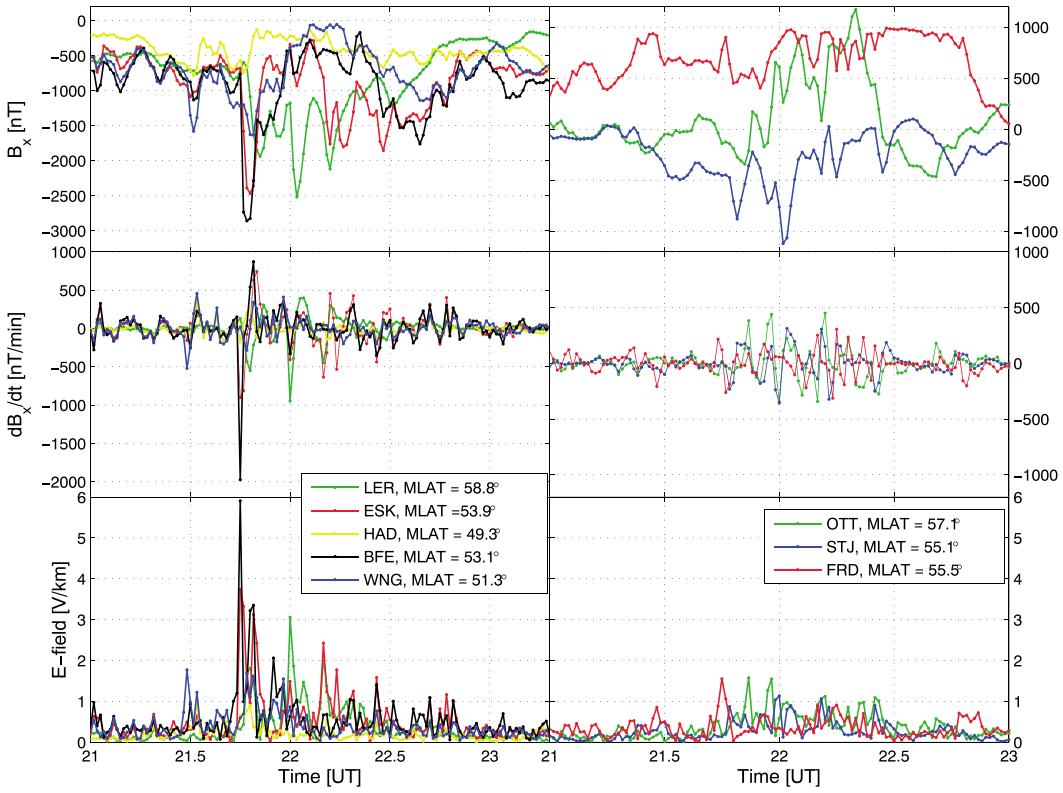

Figure 3. (top row) Geomagnetic field *X* component perturbations, (middle row) *X* component rate of change, and (bottom row) calculated geoelectric fields at selected ground magnetometer sites on 13 March 1989. The magnetometer stations are drawn from (left column) European sector and (right column) North America sector. The data in this figure at 21:46 UT correspond to the results shown in Figure 2.

locations. This is possibly related to the extension of auroral currents into the midlatitudes (as reported by *Boteler* [2001] and *Kappenman* [2005]), which is not surprising under extreme geomagnetic conditions [e.g., *Pulkkinen et al.*, 2012; *Ngwira et al.*, 2013].

3. Discussion and Conclusions

In this study we have presented two important storm cases that show that the geoelectric fields during severe storms can exhibit extreme local enhancements. Our analysis indicates that this is also true for 10 more storms identified in Table 1. A more comprehensive analysis that will take a closer examination at the other 10 storms, which is not exhaustively done in this work, and will be done in a follow-on study. As seen in Table 1 (and attached supporting information), the localized events appear at different geomagnetic latitudes ranging from as high as 85° down to around 50° and the time instances during which they occur cover a wide range of local times, suggesting that there are several physical mechanisms that can account for their existence. However, the physical processes that are responsible for the existence of these local extremes in the geoelectric field are not known. But given that the disturbances are quite localized, this implies that the source currents are also localized, which points to a source current in the ionosphere as shown by *Boteler and Jansen van Beek* [1999].

After a careful examination of the magnetic signatures provided in this study, we are led to believe that one of the possible mechanisms that might explain our results could be related to localized substorm events. The abrupt negative decrease of geomagnetic field *X* component seen at about 21:40 UT in Figure 3 is typically associated with the westward substorm electrojet. Given the intense nature of the events, it could be that the substorms occur in the temporal vicinity of the specific magnetometer stations. Substorms are perhaps one of the most dynamic process in the near-Earth space environment that provide a wealth of phenomena to study since they have a wide variety of modes in which they occur. Although only a small fraction of them cause extreme events, substorms have been recognized for a long time as one of the most geoeffective causes of large-amplitude geoelectric fields at high latitude [see, e.g., *Pulkkinen et al.*, 2005; *Viljanen et al.*, 2006b; *Ngwira et al.*, 2014, and references therein]. This is usually associated with the enhancement of the westward electrojet, a manifestation of the substorm current wedge following auroral substorm onset. It is important to note that not all cases of local enhancements are associated with strong negative *X* component deviation, but contrasting cases with positive *X* component deviation also exist, as will be demonstrated in a follow-on paper.

It is generally assumed that most intense disturbances on the ground are caused by substorms associated with the intensification of the westward auroral electrojet [e.g., *Viljanen et al.*, 2006b]. However, a previous study of the August 1972 geomagnetic storm event by *Boteler and Jansen van Beek* [1999] concluded that sudden enhancement of magnetospheric convection, due to an inward movement of the magnetopause via "erosion" rather than "compression" of the magnetosphere, caused rapid intensification of the eastward electrojet enough to produce large localized disturbances with a spatial extent of ~200 km. Historically, very little attention has been paid to the eastward electrojet, but the aforementioned study suggests that these events need to be considered as well.

Besides substorms, other important GIC drivers need to be also considered, such as geomagnetic pulsations [*Pulkkinen et al.*, 2005; *Viljanen et al.*, 1999; *Pulkkinen and Kataoka*, 2006] and sudden storm commencements [*Kappenman*, 2003; *Pulkkinen et al.*, 2005; *Fiori et al.*, 2014]. Another phenomenon worth exploring is related to transient events in the magnetosphere, i.e., bursty bulk flows (BBFs) [see, e.g., *Angelopoulos et al.*, 1992; *Grocott et al.*, 2004, and references therein]. We must caution the readers here that there are currently no studies that report on GIC effects driven by BBFs, but because of the bursty nature of these events that usually occur in association with substorms [e.g., *Grocott et al.*, 2004], we believe that there might be some connection to GIC.

Previously *Pulkkinen et al.* [2005] proposed that the fundamental nature of the storm time geoelectric field at auroral latitudes could be viewed as a multiscale process where small-scale details in source currents stipulate the exact behavior of the surface geoelectric field. Therefore, in the context of foreseeable future works, a more detailed treatment of the small-scale current structures should be considered.

Finally, we must mention that the local 3-D induction structure can also lead to localized features. Nonetheless, the localization we saw here is mostly due to the driver since the location of the peak geoelectric fields varies and occurs also at continental locations, not just at sea-land boundaries, for example. It is well known that

discontinuities in the ground conductivity structure (e.g., sea to land) can also result in localized enhancements. However, this is outside the scope of this paper.

To conclude, we would like to reiterate that our results derived from observed geomagnetic recordings show that the peak geoelectric field during severe storms are characterized, in some cases, by extreme local enhancements. However, the processes that drive these fields are not sufficiently clear. For this reason, we advocate for an interdisciplinary community-wide effort to comprehensively investigate this effect of localized fields. A detailed analysis using a multitechnique approach composed of in situ satellite-based and ground-based observations, and numerical modeling results is encouraged. Future studies should address, in-depth, the solar wind-magnetosphere-ionosphere dynamical processes that could be sources of these localized extreme geoelectric field enhancements.

Acknowledgments
We thank the national institutes that support magnetic observatories and INTERMAGNET for promoting high standards of magnetic observatory practice. Valuable discussions with Eftyhia Zesta are gratefully acknowledged. The work by C.M.N. was supported by NASA grant NNG11PL10A 670.035 to CUA/IACS and partly by ASTRA IR and D funds (grant ASTRA-2014-02 to CUA/IACS).

The Editor thanks two anonymous reviewers for their assistance in evaluating this paper.

References

Angelopoulos, V., W. Baumjohann, C. F. Kennel, F. V. Corontti, M. G. Kivelson, R. Pellat, R. J. Walker, H. Lühr, and G. Paschmann (1992), Bursty bulk flows in the inner central plasma sheet, *Geophys. Res. Lett.*, *97*(A4), 4027–4039.

Bernabeu, E. E. (2013), Modeling geomagnetically induced currents in the Dominion Virginia Power using extreme 100 year geoelectric field scenarios—Part 1, *IEEE Trans. Power Delivery*, *28*(1), 516–523.

Boteler, D. H. (2001), Space weather effects on power systems, in *Space Weather, Geophys. Monogr. Ser.*, vol. 25, edited by P. Song, H. J. Singer, and G. L. Siscoe, pp. 347–352, AGU, Washington, D. C.

Boteler, D. H., and G. Jansen van Beek (1999), August 4, 1972 revisited: A new look at the geomagnetic disturbance that caused the L4 cable system outage, *Geophys. Res Lett.*, *26*(5), 577–580.

Fiori, R. A. D., D. H. Boteler, and D. M. Gillies (2014), Assessment of GIC risk due to geomagnetic sudden commencements and identification of the current systems responsible, *Space Weather*, *12*, 76–91, doi:10.1002/2013SW000967.

Grocott, A., T. K. Yeoman, R. Nakamura, S. W. H. Cowley, H. U. Frey, H. Réme, and B. Klecker (2004), Multi-instrument observations of the ionospheric counterpart of a bursty bulk flow in the near-Earth plasma sheet, *Ann. Geophys.*, *22*, 1061–1075.

Kappenman, J. G. (2003), Storm sudden commencement events and the associated geomagnetically induced current risks to ground-based systems at low-latitude and midlatitude locations, *Space Weather*, *1*(3), 1016, doi:10.1029/2003SW000009.

Kappenman, J. G. (2005), An overview of the impulsive geomagnetic field disturbance and the power grid impacts associated with the violent Sun-Earth connection events of 29–30 October 2003 and a comparative evaluation with other contemporary storms, *Space Weather*, *3*, S08C01, doi:10.1029/2004SW000128.

Love, J. J., E. J. Rigler, A. Pulkkinen, and C. C. Balch (2014), Magnetic storms and induction hazards, *Eos Trans. AGU*, *95*(48), 445–452.

Ngwira, C. M., A. Pulkkinen, F. D. Wilder, and G. Crowley (2013), Extended study of extreme geoelectric field event scenarios for geomagnetically induced current applications, *Space Weather*, *11*, 121–131, doi:10.1002/swe.20021.

Ngwira, C. M., A. Pulkkinen, M. M. Kuznetsova, and A. Glocer (2014), Modeling extreme "Carrington-type" space weather events using three-dimensional MHD code simulations, *J. Geophys. Res. Space Physics*, *119*, 4456–4474, doi:10.1002/2013JA019661.

Pirjola, R. (2002), Review on the calculation of the surface electric and magnetic fields and geomagnetically induced currents in ground-based technological systems, *Surv. Geophys.*, *23*, 71–90.

Pulkkinen, A., and R. Kataoka (2006), S-transform view of geomagnetically induced currents during geomagnetic superstorms, *Geophys. Res. Lett.*, *33*, L12108, doi:10.1029/2006GL025822.

Pulkkinen, A., S. Lindahl, A. Viljanen, and R. Pirjola (2005), Geomagnetic storm of 29–31 October: Geomagnetically induced currents and their relation to problems in the Swedish high-voltage power transmission system, *Space Weather*, *3*, S08C03, doi:10.1029/2004SW000123.

Pulkkinen, A., E. Bernabeu, J. Eichner, C. Beggan, and A. W. P. Thomson (2012), Generation of 100-year geomagnetically induced current scenarios, *Space Weather*, *10*, S04003, doi:10.1029/2011SW000750.

Pulkkinen, A., E. Bernabeu, J. Eichner, A. Viljanen, and C. M. Ngwira (2015), Regional-scale high-latitude extreme geoelectric fields pertaining to geomagnetically induced currents, *Earth Planets Space*, *67*, 93, doi:10.1186/s40623-015-0255-6.

Tanskanen, E. I., A. Viljanen, T. I. Pulkkinen, R. Pirjola, L. Hikkinen, A. Pulkkinen, and O. Amm (2001), At substorm onset, 40% of the AL comes from underground, *J. Geophys. Res.*, *106*(A7), 13,119–13,134.

Viljanen, A., O. Amm, and R. Pirjola (1999), Modeling geomagnetically induced currents during different ionospheric situations, *J. Geophys. Res.*, *104*(A12), 28,059–28,071.

Viljanen, A., A. Pulkkinen, R. Pirjola, K. Pajunpää, P. Posio, and A. Koistinen (2006a), Recordings of geomagnetically induced currents and a nowcasting service of the Finnish natural gas pipeline, *Space Weather*, *4*, S10004, doi:10.1029/2006SW000234.

Viljanen, A., E. I. Tanskanen, and A. Pulkkinen (2006b), Relation between substorm characteristics and rapid temporal variations of the ground magnetic field, *Ann. Geophys.*, *24*, 725–733.